Dark Matter with multi-annihilation channels and AMS-02 positron excess and antiproton

Yu-Heng Chen[1], Kingman Cheung[1,2,3], and Po-Yan Tseng[1]

[1] *Department of Physics, National Tsing Hua University, Hsinchu 300, Taiwan*

[2] *Division of Quantum Phases and Devices, School of Physics, Konkuk University, Seoul 143-701, Republic of Korea*

[3] *Physics Division, National Center for Theoretical Sciences, Hsinchu, Taiwan*

(Dated: March 4, 2022)

arXiv:1505.00134v2 [hep-ph] 13 Jan 2016

Abstract

AMS-02 provided the unprecedented statistics in the measurement of the positron fraction from cosmic rays. That may offer a unique opportunity to distinguish the positron spectrum coming from various dark matter (DM) annihilation channels, if DM is the source of this positron excess. Therefore, we consider the scenario that the DM can annihilate into leptonic, quark, and massive gauge boson channels simultaneously with floating branching ratios to test this hypothesis. We also study the impacts from MAX, MED, MIN, and DC diffusion models as well as from isothermal, NFW, and Einasto DM density profiles on our results. We found two parameter regions that can satisfy both AMS-02 $\frac{e^+}{e^+ + e^-}$ and $\bar{p}/p$ datasets at 95% CL. i) Under the NFW-MIN combination with $M_\chi \subset [10, 30]$ TeV. ii) Under the Einasto-DC combination with $M_\chi \subset [500, 1500]$ GeV.

I. INTRODUCTION

Up to now the evidences of the existence of dark matter (DM) only come from the gravitational effects. In the early 1950s, people noticed the anomaly in the rotational velocity in the Milky Way and other spiral galaxies, and one logical reason is that there are non-luminous matters suffusing our universe. Currently the Planck satellite [1] pinned down that 26.8% of our universe is made up of DM. The Bullet cluster and N-body simulations may reveal some self-interaction of DM particles.

From the particle physicists' point of view, the DM particle might have interactions with the standard model (SM) particles, that will lead to interesting phenomenology. The DM direct detection experiments, like XENON100[2], CDMS II[3] etc., can probe the interactions between the DM and nucleon. Searching for the DM signal as missing energies have been performed at collider experiments such as ATLAS [4, 5] and CMS [6]. In this work, we focus on DM indirect detection. Since the DM suffuses our galaxy, they probably annihilate with each other into SM particles. In this case, the antimatters, like positrons or antiprotons, would be the ideal signals for searching for these processes, because the generation of antimatters is rare from ordinary astrophysical processes. The Alpha Magnetic Spectrometer (AMS-02) is a particle detector, which was designed to search for the antimatter and determine the composition and flux of the cosmic ray. The AMS-02 published the measurements of electron and positron results with unprecedented statistics in 2014. Their results confirmed the positron excess with energy higher than 10 GeV up to 500 GeV, which was first indicated by the PAMELA on 2008 [10, 11]. On the contrary, based on PAMELA and most recent AMS-02 [9] observation there is no significant excess of antiproton in the cosmic rays from the prediction of conventional astrophysical processes.

The DM annihilation is one of the viable interpretations for the observed positron excess, however it depends on which kinds of the SM particles that the DM particles annihilate into. The antiproton signal in general co-exists with the positron signal as parts of the annihilation products, that is severely constrained by the exisiting antiproton observations. This is one of the main difficulties in explaining the positron excess by DM annihilation. Furthermore, the newly released $\frac{e^+}{e^+ + e^-}$ data from AMS-02 has so high statistics that it may be used to distinguish various DM annihilation channels. In this work, we set up a model-independent DM annihilation framework, in which the DM could annihilate into lepton channels (e^+e^-,

μ^+, μ^-, $\tau^+\tau^-$), quark channels ($t\bar{t}$, $b\bar{b}$), and massive gauge boson channels (W^+W^-, ZZ) for a single annihilation with varying branching ratios (BR). Through fitting to the $\frac{e^+}{e^++e^-}$ and $\bar{p}/p$ data, we investigate if this DM scenario can survive, if it does, which one is the preferred channel. Here we use the $b\bar{b}$ channel to represents other lighter quark channels, because with DM mass above few hundreds GeV, the positron and anitproton spectra from $b\bar{b}$ channel are similar to those spectra from other lighter quark channels.

Note that AMS-02 very recently released the preliminary data on the ratio $\bar{p}/p$ [9], which also seems to have an unexpected rise at the first glance. However, it was shown to be consistent with the astrophysical background and conventional diffusion model within uncertainties [30–32]. We will include the most recent AMS-02 $\bar{p}/p$ data in our analysis.

This work is organized as follows. We briefly describe the AMS-02 $\frac{e^+}{e^++e^-}$ data and background models in the next section and DM model in Sec.III. The fitting results of $\frac{e^+}{e^++e^-}$ data shall be shown in Sec.IV. In Sec.V, we start considering the constraint from AMS-02 $\bar{p}/p$ data. In Sec.VI, we discuss the influences from density profiles. Then we conclude in Sec.VII.

II. AMS-02 POSITRON DATA AND BACKGROUND

In September 2014, the AMS collaboration published their high statistics measurement of the $\frac{e^+}{e^++e^-}$ in primary cosmic rays of 0.5-500 GeV [7]. The $\frac{e^+}{e^++e^-}$ increases and exceeds the astrophysical cosmic ray expectation for energy larger than about 10 GeV. This trait is consistent with the earlier observations by PAMELA [10, 11] and Fermi-LAT[12]. Furthermore, the AMS-02 provides the most precise measurement so far such that it offers more information and tighter constraints on the origin of positron excess.

The uncertainty of the high energy cosmic positron flux, which is originated from astrophysical sources and presumingly generated from the collision of high energy proton and interstellar medium (here we denote as the background), is still large. It is due to lack of knowledge of the sources and propagation models for the positron flux. The proton flux has been precisely measured by many experiments in the past and the most recently by AMS-02. The secondary electron and positron flux could be calculated straight-forwardly from the interactions of proton with interstellar material (mostly hydrogen and helium). However, there are large uncertainties in the propagation of the secondary particles from the origin of

production to the top of atmosphere (TOA). Difference diffusion models will give different positron spectra and as well as astrophysical background of $\frac{e^+}{e^+ + e^-}$ when we deal with the AMS-02 positron fraction data.

In this work, we will consider four different diffusion models, namely MIN, MED, MAX [22–24], and a diffusion convection model (DC) [25]. Each diffusion model is paired with a background, which is obtained by using the method mentioned above and computed through the Galprop package [13, 14], and these backgrounds were shown in Fig.1. More description and the parameters for these models will be given in the next section. In Fig. 1, we compare the four backgrounds of $\frac{e^+}{e^+ + e^-}$ from the four diffusion models. The ordering of background values of $\frac{e^+}{e^+ + e^-}$ is MIN > MED > MAX, when the energy $E_{e^+} \geq 10$ GeV. For the DC case, the background is close to that of MED case but has a slight deficit, when $E_{e^+} \geq 100$ GeV.

The backgrounds of $\frac{e^+}{e^+ + e^-}$ from MIN, MED, and MAX diffusion models are quite different from one another, in such a way that we anticipate that they are able to cover or represent larger portions of diffusion models in the market. Also, they are able to test whether our results are diffusion-model independent. The reason we adopt the DC diffusion model is that it utilized the more present B/C data to constrain the cosmic-ray propagation parameters.

III. POSITRON SOURCE FROM DM ANNIHILATION

The AMS-02 [7] provides a very precise measurement of the positron fraction, such that it could discriminate different DM annihilation channels and determine which one is preferred or ruled out. In order to do so, we consider the multi-annihilation channels DM scenario by assuming that the dark matter (DM) particles χ could annihilate into seven standard model (SM) channels $t\bar{t}$, $b\bar{b}$, W^+W^-, ZZ, e^+e^-, $\mu^+\mu^-$, and $\tau^+\tau^-$ from a single annihilation process. The branching ratio for each channel can float between 0 and 1, as long as they satisfy the sum rule

$$\sum_{f=t,b,W,Z,e,\mu,\tau} \mathrm{BR}(f\bar{f}) = 1\,. \tag{1}$$

The relation between the total DM annihilation cross section and each channel is specified as

$$\langle \sigma v \rangle_{\chi\bar{\chi}\to f\bar{f}} = \mathrm{BR}(f\bar{f}) \times \langle \sigma v \rangle_{tot}\ .$$

These SM particles in the final state will further decay or hadronize into positrons, antiprotons, or gamma-rays, which will be added on to the spectra obtained by the conventional high energy cosmic rays. Due to the distinctive spectral shape of these DM annihilation products, we may be able to separate these DM signals from the astrophysical cosmic rays and interpret as an indirect evidence of DM. In general, the leptonic channels e^+e^-, $\mu^+\mu^-$, and $\tau^+\tau^-$ produce a relatively harder positron energy spectrum than the quark channels $t\bar{t}$ and $b\bar{b}$. The positron spectra from massive vector boson channels W^+W^- and ZZ sit between the leptonic and quark channels.

We use the interface for model-independent analysis from micrOMEGAs [15], where the Pythia [16] was embedded to generate the positron and antiproton spectra of each DM annihilation channel. Several DM density profiles will be considered in this work, including NFW [26], isothermal [27], and Einasto [28, 29]. Nevertheless, most of the time we focus on the NFW profile. The NFW and isothermal can be parametrized by

$$\rho(r) \;=\; \rho_\odot \left\{\frac{r_\odot}{r}\right\}^\gamma \left\{\frac{1+(r_\odot/r_s)^\alpha}{1+(r/r_s)^\alpha}\right\}^{(\beta-\gamma)/\alpha} ,$$

where $\rho_\odot = 0.3\,[\mathrm{GeV/cm^3}]$ is the DM density at the Sun, $r_\odot = 8.5\,[\mathrm{kpc}]$ is the distance from the Sun to the Galactic Center (GC). The NFW (isothermal) density profile can be obtained by choosing the parameters $\alpha = 1, \beta = 3, \gamma = 1$, and $r_s = 20[\mathrm{kpc}]$ ($\alpha = 2, \beta = 2, \gamma = 0$, and $r_s = 3.5[\mathrm{kpc}]$). On the other hand, the expression for the Einasto density profile is

$$\rho(r) \;=\; \rho_s e^{\left\{-\frac{2}{\alpha}\left[\left(\frac{r}{r_s}\right)^\alpha - 1\right]\right\}} ,$$

with $\rho_s = 0.3\,[\mathrm{GeV/cm^3}]$, $r_s = 8.5\,[\mathrm{kpc}]$, and $\alpha = 0.17$, that will give $\rho(r = r_\odot) = \rho_\odot$.

In micrOMEGAs [15], the energy spectrum of the positrons is obtained by solving the diffusion-loss equation while keeping only the two dominant contributions: spatial diffusion and energy losses,

$$-\nabla\cdot(K(E)\nabla\psi_{e^+}) - \frac{\partial}{\partial E}\left(b(E)\psi_{e^+}\right) \;=\; Q_{e^+}(\mathbf{x}, E)\,, \tag{2}$$

and

$$K(E) \;=\; K_0\beta(E)(\tilde{R}/1\mathrm{GeV})^\delta\,,$$

where β and $\tilde{R} = p/q$ are the velocity and rigidity of the particle, respectively. The positron energy loss rate $b(E)$ is dominated by the synchrotron radiation in the galactic magnetic

field and by inverse Compton scattering on stellar and CMB photons. The diffusion zone of cosmic rays is represented by a cylinder with thickness $2L$ and radius R (here we use $R = 20\,[\mathrm{kpc}]$) [22]. The term Q_{e^+} on the right hand side of Eq. 2 is the positron source term.

The three diffusion models (MAX, MED, and MIN) [22–24] that we are going to consider in this work, correspond to the diffusion parameters:

$$\begin{aligned}
\mathrm{MAX}: \mathrm{L} = 15\,,[\mathrm{kpc}]\,, K_0 = 0.0765\,,[\mathrm{kpc}^2/\mathrm{Myr}]\,, \delta = 0.46\,,\\
\mathrm{MED}: \mathrm{L} = 4\,,[\mathrm{kpc}]\,, K_0 = 0.0112\,,[\mathrm{kpc}^2/\mathrm{Myr}]\,, \delta = 0.70\,,\\
\mathrm{MIN}: \mathrm{L} = 1\,,[\mathrm{kpc}]\,, K_0 = 0.0016\,,[\mathrm{kpc}^2/\mathrm{Myr}]\,, \delta = 0.85\,,
\end{aligned}$$

all of them satisfy the B/C observations. Since the AMS-02 also provided the measurement of the B/C ratio, for more comprehensive discussion of the influence of diffusion models, we add one more diffusion model, the DC model from Ref.[25], where the diffusion parameters were determined by fitting to the most recent AMS-02 B/C data.

Under the DM with the multi-annihilation-channel scenario, it will contribute to the source term Q_{e^+} in Eq. (2) through the expression

$$Q_{e^+}^{DM} \;=\; \eta \left(\frac{\rho_{DM}}{M_\chi}\right)^2 \langle\sigma v\rangle_{tot} \sum_{f=t,b,W,Z,e,\mu,\tau} \mathrm{BR}(f\bar{f})\, \frac{dN_{e^+}^f}{dE_{e^+}} \tag{3}$$

where $dN_{e^+}^f/dE_{e^+}$ is the positron energy spectrum from each annihilation event $\chi\bar{\chi} \to f\bar{f}$, and $\eta = 1/2\ (1/4)$ for (non-)identical initial state. The ρ_{DM} is the DM density profile, and M_χ is the DM mass.

IV. AMS-02 POSITRON FRACTION DATA AND FITTING RESULT

Here we attempt to use the DM scenario with multi-annihilation channels, each of which has a varying branching ratio subject to the sum rule in Eq. (1), to fit the AMS-02 $\frac{e^+}{e^+ + e^-}$ data [7]. The varying parameters are the DM mass, the annihilation cross section, and the branching ratios of seven annihilation channels: M_χ, $\langle\sigma v\rangle_{tot}$, and $\mathrm{BR}(f\bar{f})$. However, the branching ratios should satisfy the sum rule in Eq. (1), therefore, overall we have 8 free parameters.

First, we fix the DM density to the NFW profile and use various diffusion models (MIN, MED, MAX, and DC) to compute the positron flux at TOA from DM annihilation. The positron source term of DM annihilation channels can be described by Eq. (3). Then we

feed the source term into the diffusion equation (2), and it is solved numerically by the micrOMEGAs. Finally, we stack the DM-produced electron and positron flux on top of each diffusion-corresponding background flux to obtain the values of $\frac{e^+}{e^+ + e^-}$. Then we are able to compare with the AMS-02 positron fraction data.

We use the χ^2 and p-value as our statistical measures to describe the deviation of our model from the data and the goodness of the fit, respectively. [1] Our scanning strategy is fixing certain values of M_χ and $\langle \sigma v \rangle_{tot}$, meanwhile allowing the branching ratio of each channel to float as long as they satisfy the sum rule to obtain the minimal χ^2 or maximal p-value. Repeating the whole procedures to scan the parameter space of M_χ and $\langle \sigma v \rangle_{tot}$. The results are shown in Figs. 2,3,4, and 5, corresponding to MED, MAX, MIN, and DC diffusion models, respectively.

In the panel of (M_χ, $\langle \sigma v \rangle$) in each of the Figs. 2,3,4, and 5, we show the 68.3% (blue, $0.32 < p - \text{value} < 1.0$) 95% (green, $0.05 < p - \text{value} < 0.317$), and 99% (yellow, $0.01 < p - \text{value} < 0.05$) as regions of confidence level (CL) of the best-fitting points with varying branching ratios of the DM annihilation channels. In these panels, independent of the diffusion models, they show the narrow window in $\langle \sigma v \rangle_{tot}$ restricted by AMS-02 $\frac{e^+}{e^+ + e^-}$ data for each value of M_χ, despite of the variation of seven annihilation channels. Also, the total annihilation cross section $\langle \sigma v \rangle_{tot}$ strongly correlates with and is roughly proportional to the M_χ, but it is much larger than the thermal DM cross section, which is about $\langle \sigma v \rangle_{thermal} \simeq 1\,\text{pb} \simeq 3 \times 10^{-26}\text{cm}^3/\text{s}$.

In the panel of (M_χ, Br) in each of the Figs. 2,3,4, and 5, the light blue-shaded area shows the p-values of the best-fit point for the corresponding M_χ, and the $p-$value is labelled on the right-hand y-axis of the panel. It manifests itself in the (M_χ, Br) panel that once the DM mass is below 300 GeV, the p-value is always less than 0.05, independent of the diffusion models, and no matter how the combination of the annihilation channels changes. In other words, we can rule out the DM mass below 300 GeV as an explanation for the AMS-02 $\frac{e^+}{e^+ + e^-}$ excess at 95% CL. This is because the last two AMS-02 $\frac{e^+}{e^+ + e^-}$ data points with the highest energy between 260 GeV to 500 GeV cannot be explained by DM annihilation for

[1] Assuming the goodness-of-fit statistics follows χ^2 statistics, the p-value for the hypothesis is given by [21]

$$p = \int_{\chi^2}^{\infty} f(z; n) dz$$

where n is the degrees of freedom and

$$f(z; n) = \frac{z^{n/2-1} e^{-z/2}}{2^{n/2} \Gamma(n/2)} .$$

the DM mass below 300 GeV, due to the cliff shape of the positron energy spectrum from DM annihilation around M_χ. On the other hand, the upper limit for the DM mass, which are diffusion model dependent, are 5.5, 60, 50, and 13 TeV for MAX, MED, MIN, and DC, respectively.

There are two panels of (M_χ, Br) in each of the Figs. 2,3,4, and 5, one of them shows the branching ratio of individual channel for the best-fit point at the corresponding M_χ, while the other one shows the branching-ratio sum over the leptons($e^+e^- + \mu^+\mu^- + \tau^+\tau^-$), quarks($b\bar{b}$+$t\bar{t}$), or massive gauge-boson(W^+W^-+ZZ) channels. When the DM mass is below 10 TeV, the leptonic channels dominate the branching ratio (BR(leptons) $\gtrsim$ 60%), except for the region of $M_\chi < 1$ TeV in the MAX diffusion model, where the quark channels are able to compete with leptonic channels. Nonetheless, among these four diffusion models, the quark and gauge-boson channels still play non-negligible roles because (BR(gauge bosons) + BR(quarks) $\gtrsim$ 20%). Since $\langle\sigma v\rangle_{tot} \sim \mathcal{O}$ ($10^3 \sim 10^4$pb), even 10% of the W^+W^-, ZZ, and $b\bar{b}$ channels would generate enormous antiproton flux, and that is why it is severely constrained by the antiproton data [17]. Therefore, the largest p-value point for each M_χ would be ruled out by the antiproton data. Among these four diffusion models, only the MIN diffusion model at the region with $M_\chi < 350$ GeV, where the three leptonical channels can fit the AMS-02 $\frac{e^+}{e^+ + e^-}$ with $p-$value larger than 0.05. Another feature is that once the DM mass goes above 30 TeV, the $t\bar{t}$ channel becomes more and more important and eventually becomes the major channel, because of the energy spectrum of $t\bar{t}$ is relatively softer than the other channels.

In the following, we consider how the AMS-02 $\frac{e^+}{e^+ + e^-}$ data can distinguish among different channels. The panel of (M_χ, χ^2) in each of the Figs. 2,3,4, and 5 shows the chi-squares minimum with respect to M_χ if the DM can only annihilate into a single channel. The solid lines represent the single-annihilation channel scenario, while the dashed line shows the chi-square minimum of multi-annihilation channel scenario. We could see that the DM with multi-annihilation channel scenario can reduce the χ^2 significantly, although more parameters are involved. When the DM mass is less than 1 TeV, the $\tau^+\tau^-$ single-annihilation channel scenario can provide a relatively smaller value of χ^2 than the other channels, and the minimum χ^2 occurs at around M_χ =650, 800, 500, and 450 GeV for MAX, MED, MIN, and DC diffusion models, respectively. The two massive vector-boson channels attain their χ^2 minimum at about M_χ = 7, 10, 10, and 5 TeV for MAX, MED, MIN, and DC diffusion

models, respectively, because they generate moderate positron energy spectra in between the leptonic and quark channels. The $t\bar{t}$ channel, on the other hand, generates a further softer positron energy spectrum, such that the χ^2 minimum occurs at around $M_\chi = 25$, 40, 35, and 20 TeV, for the MAX, MED, MIN, and DC diffusion models, respectively. Once $M_\chi > 20$ TeV, the curve of $t\bar{t}$ is in unison with the blue-dash curve, and the $t\bar{t}$ channel takes the full responsibility for fitting the data, and other channels become irrelevant. From these results, we can see that the lepton channels are well separated from quark and massive gauge boson channels, and therefore we anticipate that the AMS-02 $\frac{e^+}{e^+ + e^-}$ data is able to distinguish the leptonic channels from the other channels in the DM multi-annihilation channel scenario. However, the χ^2 minima of W^+W^- and ZZ are almost overlapping, hence it is hard to distinguish them from each other. In the bottom-left panel of Fig. 4, with 300 GeV $\lesssim M_\chi \lesssim$ 450 GeV, pure leptonic channels are solutions of AMS-02 positron fraction data under MIN diffusion model and NFW profile.

For MIN diffusion model in Fig. 4, there is no contradiction between the panels of (M_χ, Br) and (M_χ, χ^2) around $M_\chi = 12$ TeV. At the first glance, the panel of (M_χ, χ^2) points out that the WW and ZZ channels are the most important ones to fit the data at this M_χ. However, the Br(e^+e^-) is the largest from the panel of (M_χ, Br). The reason is that the e^+e^- channel almost decouples at this DM mass region, and so the positron spectrum from it is way above the energy scale of AMS-02 $\frac{e^+}{e^+ + e^-}$ data, such that dramatically change of $\langle\sigma v\rangle_{\chi\bar{\chi}\to e^+e^-}$ does not influence the fitting too much. Therefore, the WW and ZZ channels are still the major channels to fit the data around $M_\chi = 12$ TeV.

The panel of (Br(l^+l^-), p) in Fig. 2 shows how many percentages of the leptonic channels are required to fit to the AMS-02 $\frac{e^+}{e^+ + e^-}$ data with the corresponding M_χ in the DM multi-annihilation scenario, while marginalizing all the massive gauge boson (VV) and quark ($q\bar{q}$) channels. Take M_χ= 1000 GeV, for example, the χ^2 minimum occurs with Br(l^+l^-) $\approx 75^{+20}_{-23}\%$ and Br($q\bar{q}$) + Br(VV) $\approx 25^{+23}_{-20}\%$ at 95% CL in the multi-annihilation scenario, while the single-annihilation channel scenario is the $\tau^+\tau^-$ channel but at a much larger χ^2. Two inferences we can draw from here for M_χ= 1000 GeV: (i) the major channels are the leptonic, and (ii) the three lepton channels alone, Br(l^+l^-) = 100%, could not fit well to the data. Instead, they need help from softer positron spectra of quarks or gauge bosons. When $M_\chi <$ 10 TeV, the three leptonic channels dominate. On the other hand, for $M_\chi > 10$ TeV, the VV and $q\bar{q}$ channels gradually become the major contributions. For instance, when $M_\chi =$

30 TeV, $\mathrm{Br}(l^+l^-) \approx 70^{+18}_{-70}\%$. Yet, without any lepton channels the VV and $q\bar{q}$ still have p-value = 0.3. In another words, the AMS-02 $\frac{e^+}{e^++e^-}$ data constrain more severely on the branching ratio of leptonic channels for $M_\chi < 10$ TeV.

In Fig. 6, we would like to demonstrate how different background of $\frac{e^+}{e^++e^-}$ originating from different diffusion models will modify the conclusions that we made in previous paragraph. For all three diffusion models MAX, MED, and MIN at $M_\chi \simeq 1$ TeV, the values of $\mathrm{Br}(l^+l^-)$ are still confined in a narrower window with about $\pm 20\%$ deviation at 95% CL from the best-fit value of $\mathrm{Br}(l^+l^-)$. On the other hand, for $M_\chi > 10$ TeV the confinement is much loose such that the values of $\mathrm{Br}(l^+l^-)$ can go down to zero in MED and MIN cases. Another feature we can see from this figure is that in the MIN (MAX) diffusion model, the values of $\mathrm{Br}(l^+l^-)$ concentrate at slightly larger (smaller) values than those of the MED model.

V. AMS-02 ANTIPROTON-PROTON RATIO DATA AND FITTING RESULTS

During 15-17 April 2015 at CERN Geneva, the AMS collaboration presented the preliminary results on the spectrum of the antiproton-to-proton ratio for proton kinetic energy (KE) up to 450 GeV [9], with much higher precision than other measurements in the past. The data points with KE between 20 and 450 GeV show a flat structure. Comparing the AMS-02 and PAMELA $\bar{p}/p$ data, with KE larger than 5 GeV up to 180 GeV, these two datasets are consistent within the errors.

The derivation of the antiproton background is analogous to the positron case. First, we specify the diffusion model and determine the proton flux from the data, then compute the antiproton flux based on Galprop [13, 14]. Various backgrounds originating from the corresponding diffusion models are shown in Fig. 7. There is a moderate excess of the AMS-02 $\bar{p}/p$ data above various backgrounds. Comparing among these four backgrounds, the one from the DC diffusion model provides a slight better fit to the AMS-02 $\bar{p}/p$ data.

We keep four annihilation channels ($t\bar{t}$, $b\bar{b}$, W^+W^-, and ZZ) of DM for the the calculation of antiproton ratio, because these channels can generate antiprotons after decay and hadronization, while the e^+e^- and $\mu^+\mu^-$ channels are irrelevant and the contribution from the $\tau^+\tau^-$ channel is negligible. We therefore define $\langle\sigma v\rangle_{\bar{p}/p} \equiv \sum_{f\bar{f}=t\bar{t},b\bar{b},WW,ZZ} \langle\sigma v\rangle_{\chi\bar{\chi}\to f\bar{f}}$. We take this multi-annihilation DM scenario to fit to the AMS-02 $\bar{p}/p$ data, and use only the data with KE larger than 5 GeV in the fitting. The results in terms of CL regions in the

(M_χ, $\langle\sigma v\rangle$) panels with MAX, MED, MIN, and DC diffusion models are shown in Fig. 8.

In Fig. 8, we can see a strong and almost linear correlation between M_χ and $\langle\sigma v\rangle_{\bar{p}/p}$ in all four panels. The 95% CL lower and upper limits on M_χ depends on the diffusion-model. The 95% lower limit on M_χ = 850, 600, 1000, and 450 GeV for MAX, MED, MIN, and DC diffusion models, respectively. The value of $\langle\sigma v\rangle_{\bar{p}/p}$ required to fit the AMS-02 $\bar{p}/p$ data is always smaller than the $\langle\sigma v\rangle_{tot}$ required to fit the AMS-02 $\frac{e^+}{e^++e^-}$ data with the corresponding M_χ, except for the MIN diffusion model with $M_\chi \geq 10$ TeV. Nevertheless, the values of $\langle\sigma v\rangle_{tot}$ and $\langle\sigma v\rangle_{\bar{p}/p}$ are of the same order of magnitude. The values of $\langle\sigma v\rangle_{\bar{p}/p}$ for the MIN diffusion model are about two orders of magnitude larger than the other models, mainly because of the fact that the diffusion zone of MIN is thinner than the other diffusion models such that particles are easier to escape the diffusion zone during propagation. It then requires larger values of $\langle\sigma v\rangle_{\bar{p}/p}$ to compensate for the lost particles. Thus, for $M_\chi \geq 10$ TeV the value of $\langle\sigma v\rangle_{\bar{p}/p}$ for the MIN diffusion model is of the same order as the value of $\langle\sigma v\rangle_{tot}$ in Fig. 4. In other words, in the NFW-MIN case for $M_\chi \geq 10$ TeV, it can tolerate large branching ratios of massive vector boson and quark channels without conflict with the upper bound from AMS-02 $\bar{p}/p$ data.

The 95% CL upper limit on $\langle\sigma v\rangle_{\bar{p}/p}$ shown in Fig. 8 are also diffusion-model dependent. Taking the MED diffusion model as an example with $M_\chi = 1(10)$ TeV, the upper limit on $\langle\sigma v\rangle_{\bar{p}/p} \approx 20$ (1000) pb, which is about 1/30 of the favored value of $\langle\sigma v\rangle_{tot}$ in the AMS-02 $\frac{e^+}{e^++e^-}$ case. In other words, if we try to fit both AMS-02 $\bar{p}/p$ and $\frac{e^+}{e^++e^-}$ data, the $\mathrm{BR}(\bar{q}q) + \mathrm{BR}(VV) \lesssim 3\%$ or $\mathrm{Br}(l^+l^-) \gtrsim 97\%$ is required. However the panel of (Br(l^+l^-), p) in Fig. 2 tells us that the parameter region satisfying the above requirement is very narrow: only when $M_\chi \lesssim 1$ TeV and the $p-$value is less than 0.1. After scrutinizing the parameter space of the multi-annihilation channel DM scenario, it cannot provide simultaneously good fits to both the AMS-02 $\frac{e^+}{e^++e^-}$ and $\bar{p}/p$ data with a $p-$value larger than 0.05 based on the NFW-MED combination.

A simultaneous solution for both AMS-02 $\frac{e^+}{e^++e^-}$ and $\bar{p}/p$ data could be found under the NFW-MIN combination for $M_\chi \subset [10, 30]$ TeV, as shown by the compensating color in the panel of (M_χ, $\langle\sigma v\rangle$) in Fig. 4. The upper two panels in Fig. 11 show the a benchmark point of the solution for both AMS-02 $\frac{e^+}{e^++e^-}$ and $\bar{p}/p$ data, with both p-values larger than 0.05: $M_\chi = 23$ TeV with composition of 22% $\tau^+\tau^-$, 39% $t\bar{t}$, and 39% ZZ channels.

After the comprehensive parameter survey of the multi-annihilation channel DM, we did

not find any solution to simultaneously explain the AMS-02 $\frac{e^+}{e^+ + e^-}$ and $\bar{p}/p$ data under the case of the NFW profile combined with MAX, MED, or DC diffusion models.

VI. DIFFERENT DARK MATTER DENSITY PROFILES

So far in the above sections, we only focus on the NFW DM density profile. In this section, we investigate the consequences of using different density profiles by adopting the isothermal and Einasto profiles.

Among these profiles, we have normalized the DM density to $\rho(r_\odot = 8.5\,\mathrm{kpc}) = 0.3\,\mathrm{GeVcm}^{-3}$ at our solar system, where $r_\odot$ is the distance of our solar system from the GC. Note that the largest uncertainty among various profiles happens within 1 kpc around the GC. Around the vicinity of our solar system, the isothermal and NFW profiles are almost identical, but however some deviations between Einasto and NFW happens. Hence, the positron spectra from DM annihilation from isothermal and NFW profiles are quite similar, but different from the Einasto profile. In general, the Einasto profile will give a softer positron spectrum than the NFW and isothermal. This feature could make it easier for the multi-annihilation channel DM scenario to fit simultaneously to both AMS-02 $\frac{e^+}{e^+ + e^-}$ and $\bar{p}/p$ data, because the missing ingredient in the NFW profile is that the positron spectrum from leptonic channels is not soft enough for the $\frac{e^+}{e^+ + e^-}$ data. In the following, we take the combination of the Einasto profile and the DC diffusion model to demonstrate this feature, since the DC model utilizes a more recent B/C observation to constrain their cosmic-ray propagation parameters.

Based on the Einasto-DC combination, the AMS-02 $\frac{e^+}{e^+ + e^-}$ and $\bar{p}/p$ fitting results are shown in Figs. 9 and 10, respectively. The benchmark point of multi-annihilation channel DM that can explain both data sets is illustrated in the lower two panels of Fig. 11. Comparing the Fig. 5 (NFW) with Fig. 9 (Einasto), larger values of $M_\chi > 10$ TeV are allowed at 95% CL in the Einasto profile. From the panels of (M_χ, χ^2), the fitting of the single channels of $\tau^+\tau^-$, VV and $\bar{q}q$ are all improved in the Einasto profile than those in NFW one. Also, because of the improvement in VV and $\bar{q}q$ channels, the region of $M_\chi > 10$ TeV is allowed. Another difference in the panels of (M_χ, χ^2) between these two profiles is that the corresponding values of M_χ of the minimum of each channel shifts to larger values in the Einasto case. This comes from the fact that the Einasto profile makes positron spectra

from each channels softer. In the panels of (M_χ, Br) in Fig. 9, when M_χ less than 1200 GeV, the Br(l^+l^-) of the best-fit point can be larger than 95%, and so Br(VV) + Br($\bar{q}q$) is suppressed below 5%. This region provides a nice habitat to accommodate the AMS-02 $\bar{p}/p$ data. In the panel of (M_χ, $\langle\sigma v\rangle$), the red long-elliptical contour indicates the allowed DM mass and annihilation cross section that can explain well these two AMS-02 observations. The DM mass range is $M_\chi \subset [500, 1500]$ GeV.

In Fig. 10, we show the results of fitting to the AMS-02 $\bar{p}/p$ data under the Einasto-DC combination. Comparing the panel of (M_χ, $\langle\sigma v\rangle$) in this figure to the bottom-right panel (corresponding to the NFW-DC combination) in Fig. 8, the 95% CL allowed range for DM mass does not change much, 400 GeV $\lesssim M_\chi \lesssim$ 15 TeV. However, because of the DM density $\rho(r)$ of the Einasto profile is larger than that of NFW for $r \leq r_\odot$, the entire CL region shifts down by a factor of 2 for the Einasto case, indicating that the value of $\langle\sigma v\rangle_{tot}$ for the Einasto case is half of that for NFW. Similar observation can be seen from the fitting to the AMS-02 $\frac{e^+}{e^+ + e^-}$ data, by comparing the panels of (M_χ, $\langle\sigma v\rangle$) in Figs. 5 and 9. Another observation from the two panels of (M_χ, Br) in Fig. 10 for the best-fit point is that when $M_\chi \lesssim 1700$ GeV, the massive gauge boson channels take the most responsibility to fit the data. However, when $M_\chi \gtrsim 1700$ GeV, the quark channels take over the major role to do the fitting.

In summary, the two major differences between the Einasto and NFW profiles are (i) the former makes the positron spectra from DM annihilation softer than the latter, and (ii) in order to produce the same amount of positron or antiproton flux from DM annihilation, a slightly smaller annihilation cross section is required in the Einasto profile.

VII. CONCLUSIONS

In this work, we have postulated a DM scenario with multi-annihilation channels to account for the positron fraction excess and antiproton-to-proton ratio observed in cosmic rays. By using the most updated $\frac{e^+}{e^+ + e^-}$ and $\bar{p}/p$ data from AMS-02, we have performed a comprehensive analysis to determine the preferred DM annihilation channel in terms of statistic quantities χ^2 and p-values. We have considered the DM annihilation into $t\bar{t}$, $b\bar{b}$, W^+W^-, ZZ, e^+e^-, $\mu^+\mu^-$, and $\tau^+\tau^-$ channels from a single annihilation process, and taken the branching ratio of each channel and the total cross section as the fitting parameters. We

focus on two aspects: i) Which channel is preferred by the AMS-02 $\frac{e^+}{e^++e^-}$ data, and how strong the confinement of branching ratios can be implied. ii) Under this multi-annihilation channel DM scenario, we are looking for a simultaneous solution for both AMS-02 $\frac{e^+}{e^++e^-}$ data and $\bar{p}/p$ data. Several diffusion models (MAX, MED, MIN, and DC) and DM density profiles (isothermal, NFW, Einasto) are invstigated in our analysis. Uncertainties in astrophysical backgrounds are obtained via combinations of various density profiles and diffusion models.

Our findings are summarized as follows.

1. The allowed region of DM mass M_χ and annihilation cross sections $\langle\sigma v\rangle_{tot}$ that can provide good fits with p-value ≥ 0.05 to the AMS-02 $\frac{e^+}{e^++e^-}$ data is very broad. The range of M_χ extends from 300 GeV to a few tens of TeV, and $\langle\sigma v\rangle_{tot}$ extends from $O(100)$ pb to $O(10^5)$ pb. However, there is strong and almost linear correlation between the M_χ and $\langle\sigma v\rangle_{tot}$.

2. The DM mass below 300 GeV is ruled out at 95% CL by the $\frac{e^+}{e^++e^-}$ data, and this lower limit of M_χ is diffusion-model and density-profile independent. On the other hand, the upper limit for the DM mass strongly depends on the diffusion models and density profiles. Pure leptonic channels are solutions of AMS-02 positron fraction data under combination of NFW-MIN with $M_\chi \subset [300, 450]$ GeV or combination of Einasto-DC with $M_\chi \subset [300, 1800]$ GeV.

3. The high statistical measurement from AMS-02 has the capacity to distinguish among different annihilation channels. For a few hundred GeV to several TeV DM, the $\tau+\tau^-$ channel is the ideal one to fit to the $\frac{e^+}{e^++e^-}$ data. On the other hand, for several TeV to 10 TeV DM, the W^+W^- and ZZ are the favorites. Beyond 10 TeV the $b\bar{b}$ and $t\bar{t}$ channels begin to take over and completely dominate very quickly.

4. Based on the multi-annihilation channel DM scenario, for all MAX, MED, and MIN diffusion models, when $M_\chi \simeq 1$ TeV, the AMS-02 $\frac{e^+}{e^++e^-}$ data has the best confinement of the branching ratio of the sum of three leptonic channels, and Br(l^+l^-) is within $\pm 20\%$ deviation from the best-fit value at 95% CL. However, the value of Br(l^+l^-) for the best-fit point depends on the diffusion model.

5. The DM scenario with multi annihilation channels under the combinations of the MAX, MED and DC diffusion models, and the NFW density profile cannot satisfy

both AMS-02 $\frac{e^+}{e^+ + e^-}$ and $\bar{p}/p$ data at 95% CL. However, under the NFW-MIN and Einasto-DC combinations, we find windows in, respectively, $M_\chi \subset [10, 30]$ TeV and $M_\chi \subset [500, 1500]$ GeV that can fit well with p-value ≥ 0.05 to both datasets, For the Einasto-DC case, the $\tau^+\tau^-$ channel dominates and the massive gauge boson and quark channels are suppressed. On the other hand, for the NFW-MIN case the ZZ and $t\bar{t}$ are the two major channels.

During the last stage of the manuscript, we came across a few similar works in model-independent approach [30, 33–35] and in specific models [36, 37].

ACKNOWLEDGMENT

This work was supported by the MoST of Taiwan under Grants No. 102-2112-M-007-015-MY3.

---

[1] Planck Collaboration (P.A.R. Ade (Cardiff U.) *et al.*), Astron. Astrophys. **571** (2014) A16, [astro-ph.CO/1303.5076].

[2] XENON100 Collaboration (E. Aprile (Columbia U.) *et al.*), Phys. Rev. Lett. **109** (2012) 181301, [astro-ph.CO/1207.5988].

[3] CDMS Collaboration (R. Agnese (Florida U.) *et al.*), Phys. Rev. Lett. **111** (2013) 25, 251301, [hep-ex/1304.4279].

[4] ATLAS Collaboration (Georges Aad (Freiburg U.) *et al.*), JHEP. **1304** (2013) 075, [hep-ex/1210.4491].

[5] ATLAS Collaboration (Georges Aad (Freiburg U.) *et al.*), Phys. Rev. Lett. **110** (2013) 1, 011802, [hep-ex/1209.4625].

[6] CMS Collaboration (Serguel Chatrchyan (Yerevan Phys. Inst.) *et al.*), JHEP. **1209** (2012) 094, [hep-ex/1206.5663].

[7] AMS Collaboration (L. Accardo *et al.*), Phys. Rev. Lett. **113**, 121101 (2014).

[8] AMS Collaboration (M. Aguilar *et al.*), Phys. Rev. Lett. **113**, 121102 (2014).

[9] AMS Collaboration, Talks at the "AMS Days at CERN", 15-17 April 2015, "http://press.web.cern.ch/press-releases/2015/04/physics-community-discuss-latest-results-

ams-experiment."

[10] PAMELA Collaboration (O. Adriani *et al.*), Phys. Rev. Lett. **111**, (2013) 8, 081102, [astro-ph/1308.0133].

[11] PAMELA Collaboration (O. Adriani (Florence U. & INFN, Florence) *et al.*), Nature **458**, (2009) 607-609, [astro-ph/0810.4995].

[12] Fermi LAT Collaboration (M. Ackermann *et al.*), Phys. Rev. Lett. **108**, (2012) 011103, [astro-ph/1109.0521].

[13] A. W. Strong and I. V. Moskalenko, Astrophys. J. **509**, 212 (1998) [astro-ph/9807150].

[14] I. V. Moskalenko and A. W. Strong, Astrophys. J. **493**, 694 (1998) [astro-ph/9710124].

[15] G. Belanger, F. Boudjema, A. Pukhov, and A. Semenov, https://lapth.cnrs.fr/micromegas/ .

[16] T. Sjostrand, S. Ask, J. R. Christiansen, R. Corke, N. Desai, P. Ilten, S. Mrenna, S.Prestel, C. O. Rasmussen, P. Z. Skands, http://home.thep.lu.se/∼torbjorn/Pythia.html .

[17] PAMELA Collaboration (O. Adriani *et al.*), Phys. Rev. Lett. **105**, (2010) 121101, [astro-ph/1007.0821].

[18] M.N. Mazziotta, F. Loparco, [astro-ph.HE/1302.5359].

[19] David Maurin, R. Taillet, C. Combet, [astro-ph/0609522].

[20] Alejandro Lopez, Christopher Savage, Douglas Spolyar, Douglas Q. Adams, [astro-ph/1501.01618].

[21] J. Beringer et al. (Particle Data Group), Phys. Rev. **D86**, 010001 (2012).

[22] T. Delahaye, R. Lineros, F. Donato, N. Fornengo, P. Salati, Phys. Rev. **D77**, (2008) 063527, [asto-ph/0712.2312].

[23] D. Maurin, F. Donato, R. Taillet, and P. Salati, Astro- phys. J. **555**, 585 (2001).

[24] F. Donato, N. Fornengo, D. Maurin, P. Salati, and R. Taillet, Phys. Rev. **D69**, 063501 (2004).

[25] S. J. Lin, X. J. Bi, P. F. Yin and Z. H. Yu, arXiv:1504.07230 [hep-ph].

[26] J. F. Navarro, C. S. Frenk and S. D. M. White, Astrophys. J. **462**, 563 (1996), [astro-ph/9508025].

[27] A. Burkert, IAU Symp. 171, 175 (1996) [Astrophys. J. **447**, L25 (1995)], [astro-ph/9504041].

[28] J. F. Navarro, A. Ludlow, V. Springel, J. Wang, M. Vogelsberger, S. D. M. White, A. Jenkins and C. S. Frenk *et al.*, [arXiv:0810.1522].

[29] A. W. Graham, D. Merritt, B. Moore, J. Diemand and B. Terzic, Astron. J. **132**, 2685 (2006), [astro-ph/0509417].

[30] Galle Giesen, Mathieu Boudaud, Yoann Genolini, Vivian Poulin, Marco Cirelli, Pierre Salati, Pasquale D. Serpico, Jie Feng, Antje Putze, Sylvie Rosier-Lees *et al.*, [astro-ph.HE/1504.04276].

[31] C. Evoli, D. Gaggero and D. Grasso, arXiv:1504.05175 [astro-ph.HE].

[32] R. Kappl, A. Reinert and M. W. Winkler, arXiv:1506.04145 [astro-ph.HE].

[33] H. B. Jin, Y. L. Wu and Y. F. Zhou, arXiv:1504.04604 [hep-ph].

[34] K. Hamaguchi, T. Moroi and K. Nakayama, arXiv:1504.05937 [hep-ph].

[35] S. J. Lin, X. J. Bi, P. F. Yin and Z. H. Yu, arXiv:1504.07230 [hep-ph].

[36] M. Ibe, S. Matsumoto, S. Shirai and T. T. Yanagida, arXiv:1504.05554 [hep-ph].

[37] C. H. Chen, C. W. Chiang and T. Nomura, arXiv:1504.07848 [hep-ph].

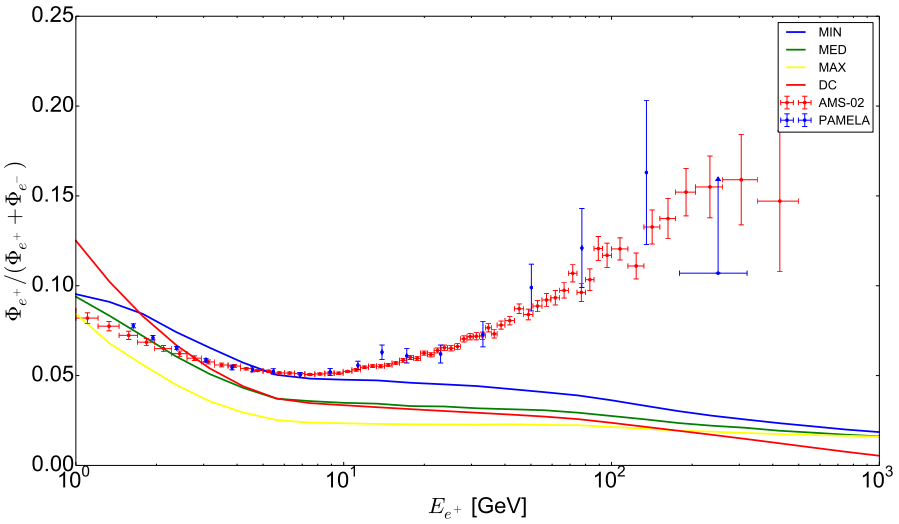


FIG. 1. The astrophysical backgrounds for the observable of $\Phi_{e^+}/(\Phi_{e^-}+\Phi_{e^+})$ using different diffusion models, corresponding to the MIN, MED, MAX, and DC diffusion models. Red crosses are the AMS-02 $\frac{e^+}{e^-+e^+}$ data [7] and blue crosses are the PAMELA $\frac{e^+}{e^-+e^+}$ data [10, 11].

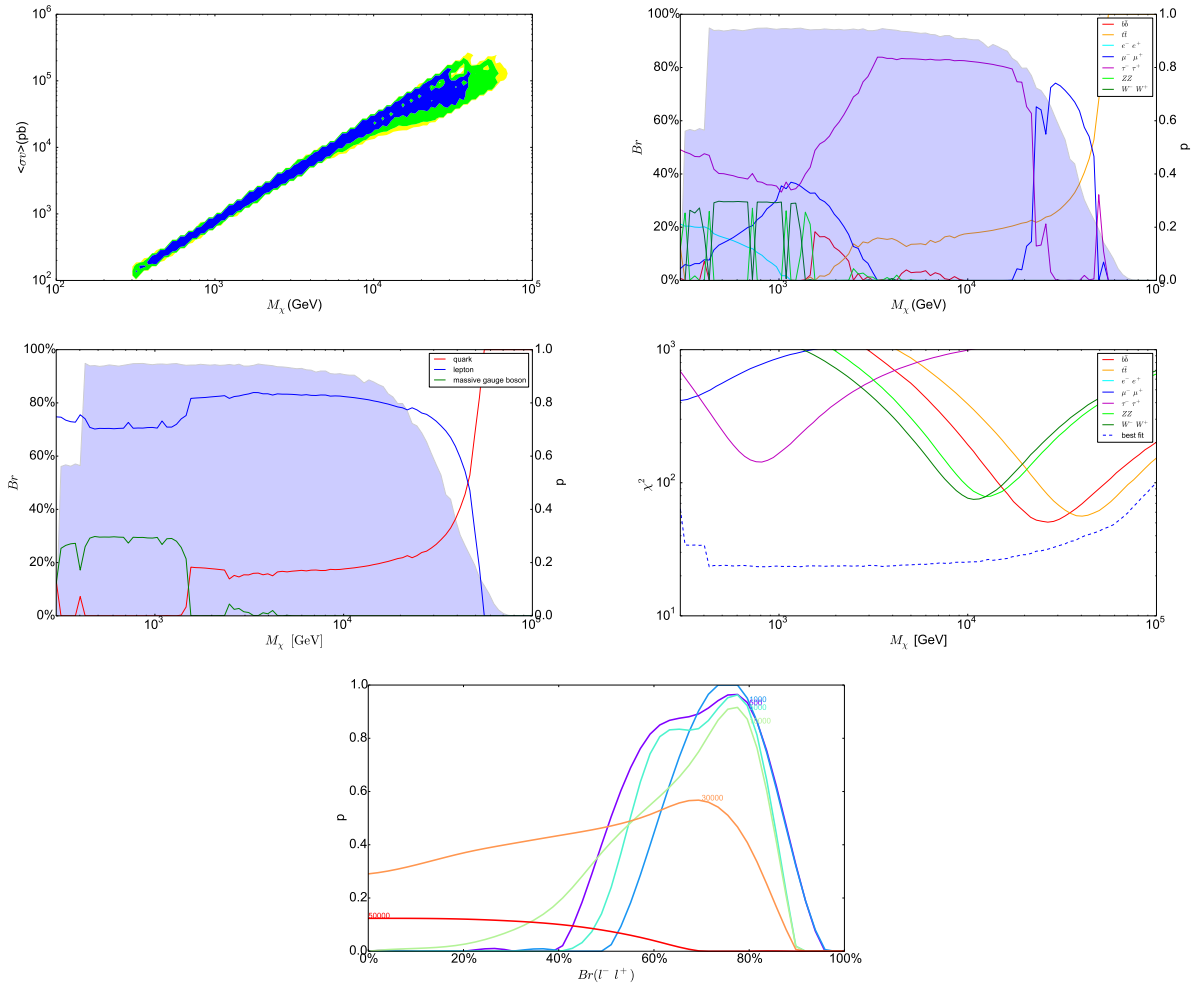


FIG. 2. Fitting results of the multi-annihilation channel DM scenario to AMS-02 $\frac{e^+}{e^-+e^+}$ data for the combination of *NFW-MED*. Description goes from top to bottom and from left to right. i) Upper-left: the allowed region in the plane of $(M_\chi, \langle\sigma v\rangle)_{tot}$. The blue region indicates $0.32 < p-$value < 1.0 (68.3% CL), the green region $0.05 < p-$value < 0.317 (95% CL), and the yellow region $0.01 < p-$value < 0.05 (99% CL). ii) Upper-right: (M_χ, BR). The branching ratio of each channel for the best-fit points, labelled on the left y-axis. The blue-shaded region is the $p-$value of the best-fit points labelled on the right y-axis. iii) Middle-left: (M_χ, Br). Same as ii), but for summing over the leptonic, quark, and massive gauge boson channels. iv) Middle-right: (M_χ, χ^2). Each of the solid curves shows the χ^2 in the fitting to the AMS-02 $\frac{e^+}{e^-+e^+}$ data using only a single DM annihilation channel, namely, $b\bar{b}$, $t\bar{t}$, e^-e^+, $\mu^-\mu^+$, $\tau^-\tau^+$, ZZ, or W^-W^+. The dashed curve represents the χ^2 from the multi-annihilation channel DM scenario. v) Lower: (Br(l^-l^+), p). The sum of leptonic branching ratios $\mathrm{Br}(l^-l^+) \equiv \sum_{f=e,\mu,\tau} \mathrm{Br}(f\bar{f})$ vs the p-values for a number of M_χ values, labelled right next to the curves while marginalizing all other fitting parameters.

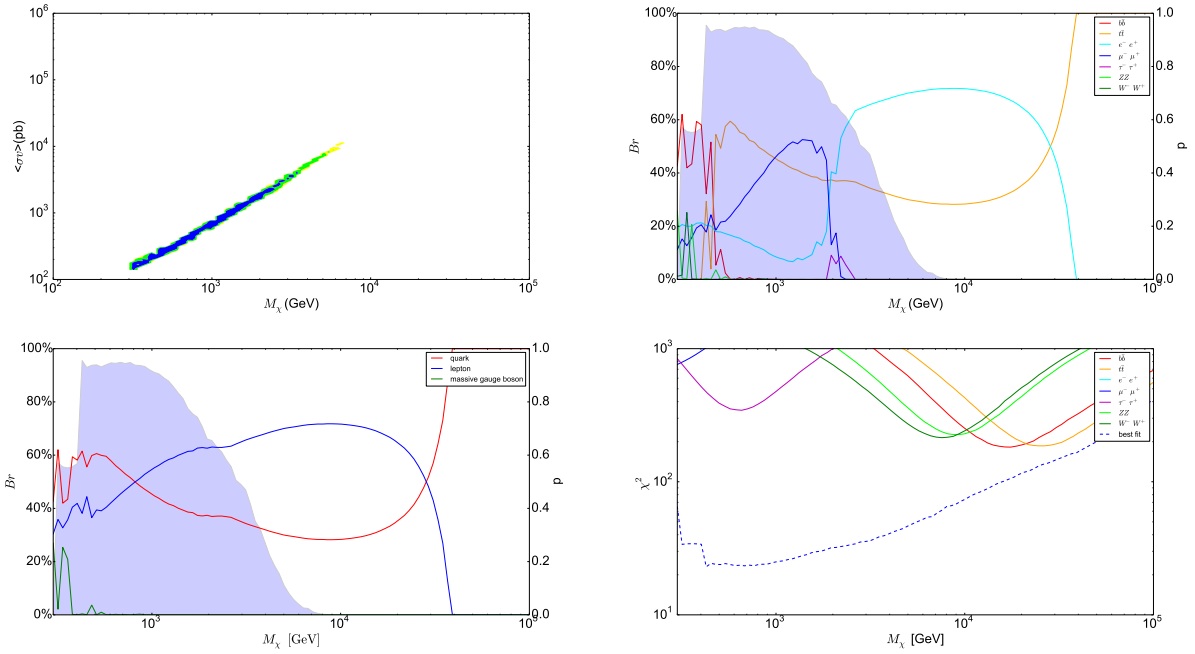


FIG. 3. The same as Fig. 2 but for the combination of of NFW-MAX, except without the last panel.

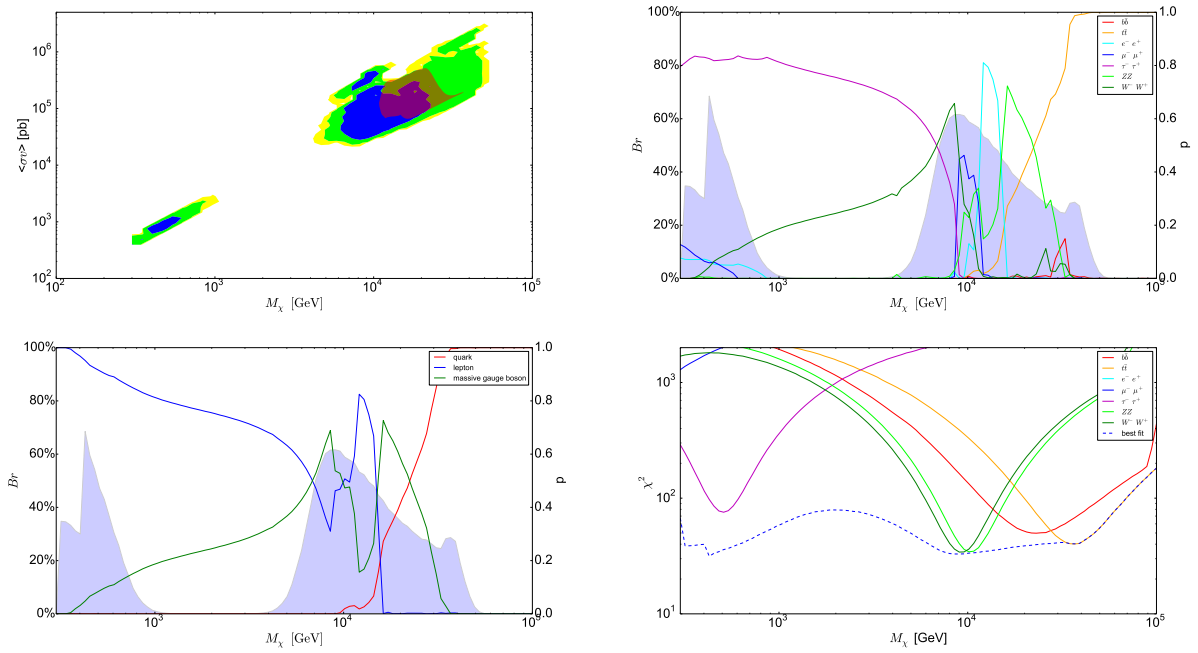


FIG. 4. The same as Fig. 2 but for the combination of of NFW-MIN, except without the last panel. The compensating color in upper-left panel in the plane of (M_χ, $\langle\sigma v\rangle$) shows the allowed region of fitting simultaneously to both AMS-02 $\frac{e^+}{e^-+e^+}$ and $\bar{p}/p$ data with p-value > 0.05 for each dataset.

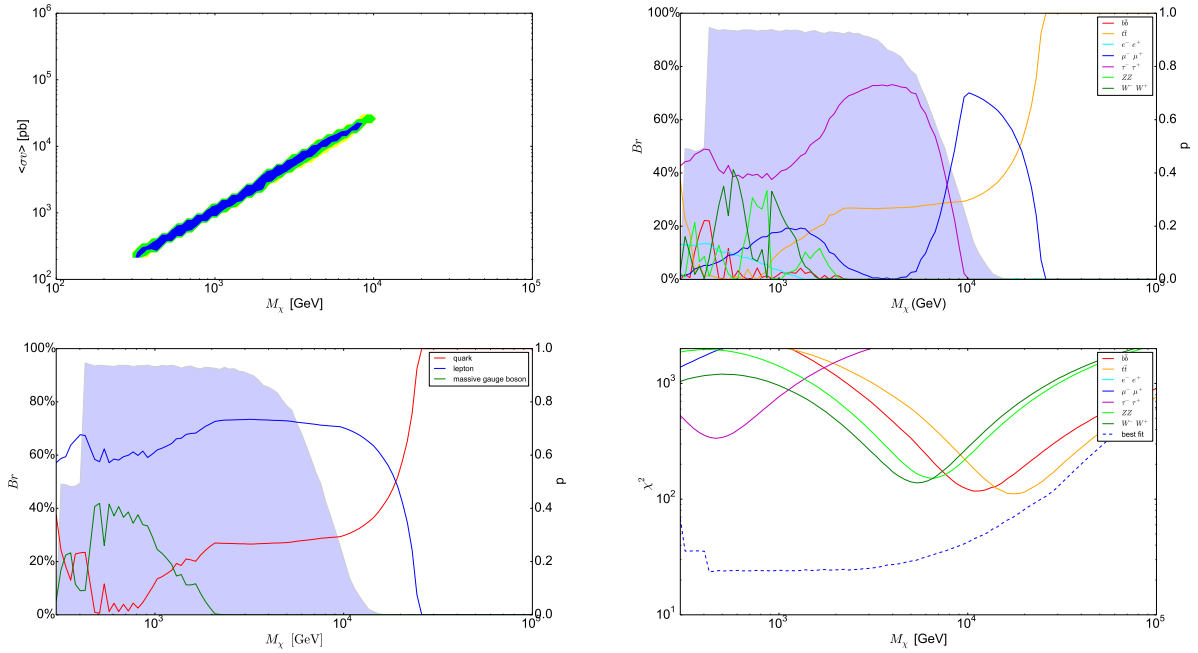


FIG. 5. The same as Fig. 2 but for the combination of of NFW-DC, except without the last panel.

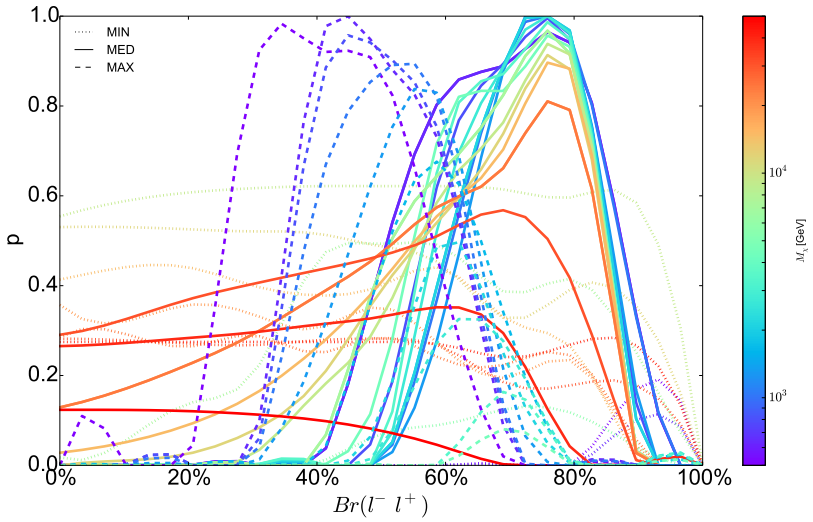


FIG. 6. The same description as the lower panel in Fig. 2, except for using all different diffusion models. MIN: dotted curves; MED: solid curves; MAX: dashed curves. The color bar on the right-hand side indicates the DM mass M_χ.

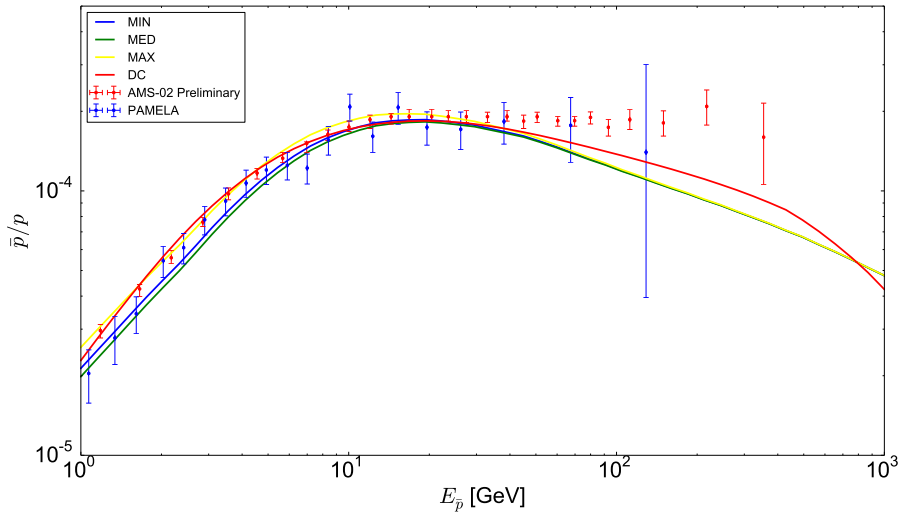


FIG. 7. Astrophysical backgrounds for the observable $\bar{p}/p$ data with the MIN, MED, MAX, and DC diffusion models. The red dots are the AMS-02 $\bar{p}/p$ preliminary data. The blue dots are the PAMELA $\bar{p}/p$ data.

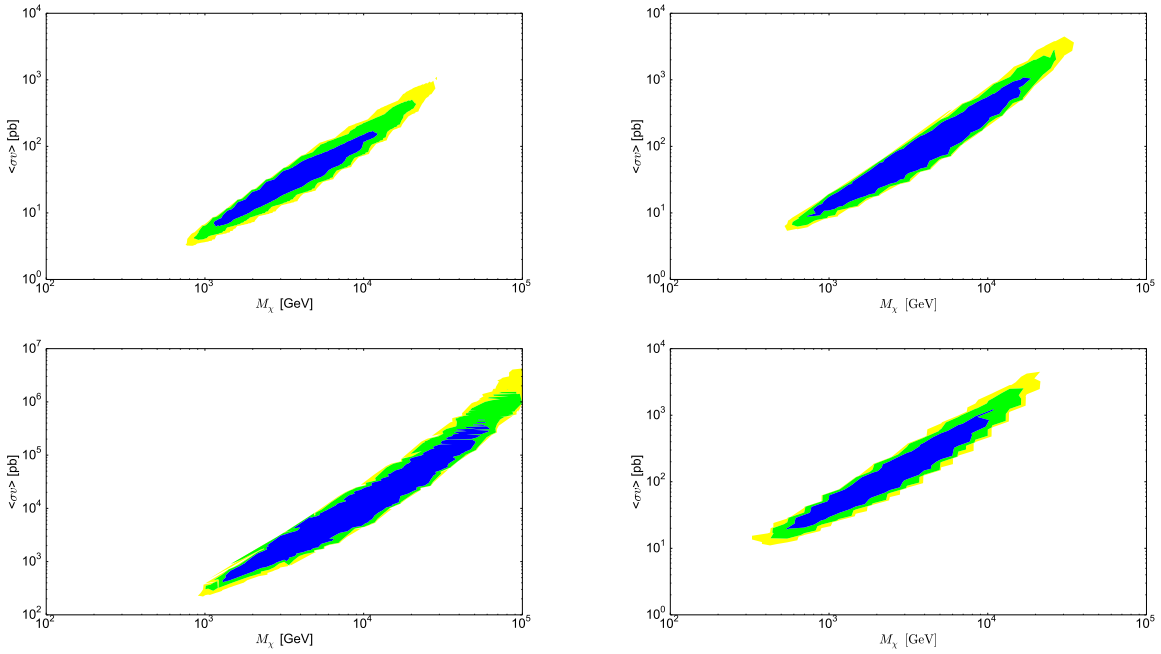


FIG. 8. The fitting results in the plane of $(M_\chi, \langle\sigma v\rangle)$ of the multi-annihilation channel DM scenario to the AMS-02 $\bar{p}/p$ data. The relevant channels are $t\bar{t}$, $b\bar{b}$, W^+W^-, and ZZ: $\langle\sigma v\rangle = \sum_{f=t,b,W,Z} \langle\sigma v\rangle_{\chi\bar{\chi}\to f\bar{f}}$. The blue region indicates $0.32 < p-$value < 1.0 (68.3% CL), the green region $0.05 < p-$value < 0.317 (95% CL), and the yellow region $0.01 < p-$value < 0.05 (99% CL). The panels are: upper-left for the combination of NFW-MAX, upper-right for NFW-MED, bottom-left for NFW-MIN, and bottom-right for NFW-DC.

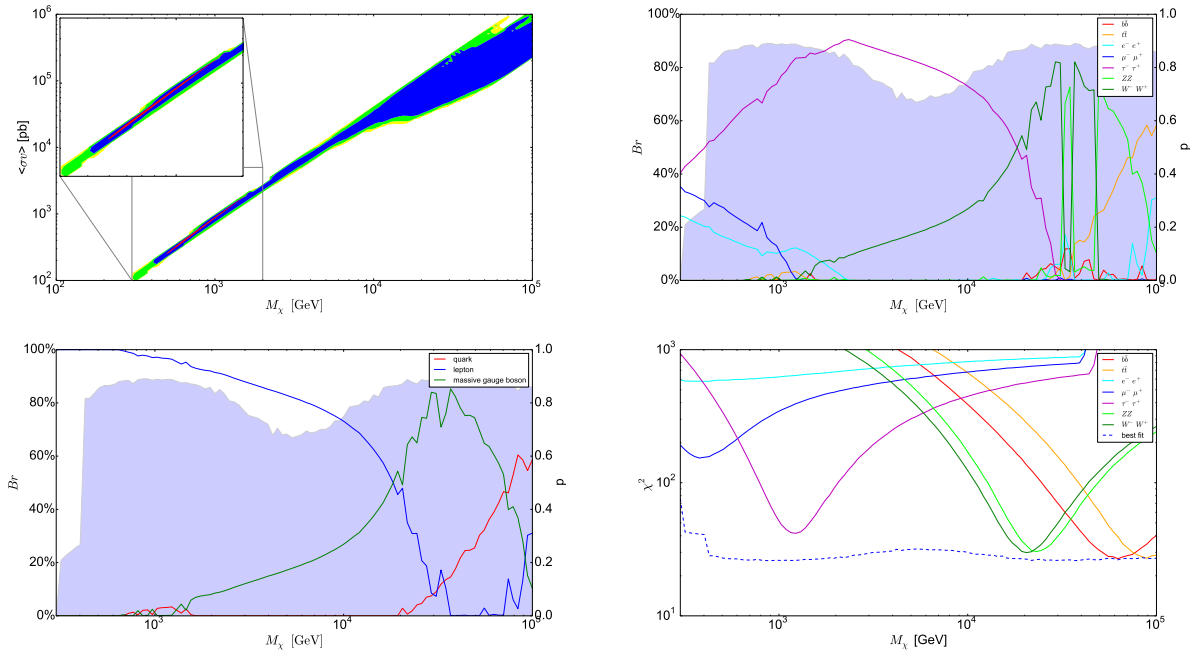


FIG. 9. The same as Fig. 2 but for the combination of of Einasto-DC, except without the last panel. The red region in the upper-left panel in the plane of (M_χ, $\langle\sigma v\rangle$) shows the allowed region of simultaneously fitting to both AMS-02 $\frac{e^+}{e^-+e^+}$ and $\bar{p}/p$ datasets with p-value > 0.05 for each dataset. A zoom is displaced in the upper-left corner of that panel.

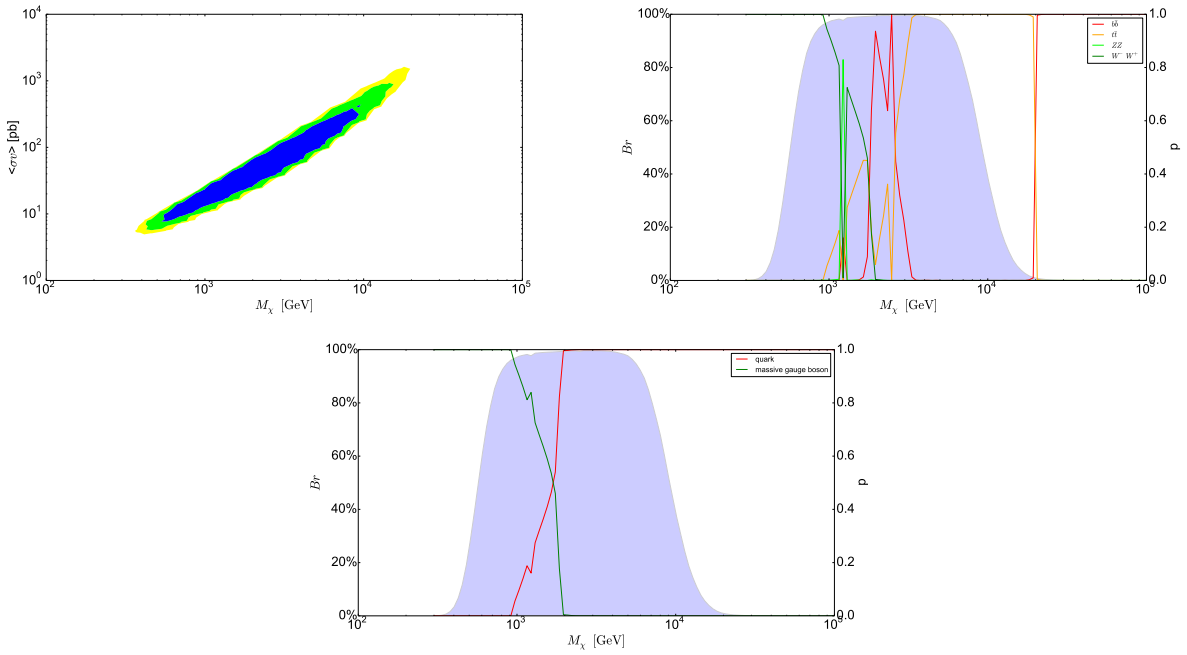


FIG. 10. Fitting results using the combination of Einasto-DC with respect to the AMS-02 $\bar{p}/p$ data. Upper-left: (M_χ, $\langle\sigma v\rangle$) – confidence-level regions, labeled in the same way as Fig. 8. Upper-right: (M_χ, Br) – fitting to the AMS-02 $\bar{p}/p$ data alone with $t\bar{t}$, $b\bar{b}$, W^+W^-, and ZZ channels. Lower: (M_χ, Br) – similar to the upper-right one, but summing over the similar channels: quark $= \sum_{f=b,t} \mathrm{Br}(f\bar{f})$ and massive gauge boson $= \sum_{f=W,Z} \mathrm{Br}(f\bar{f})$.

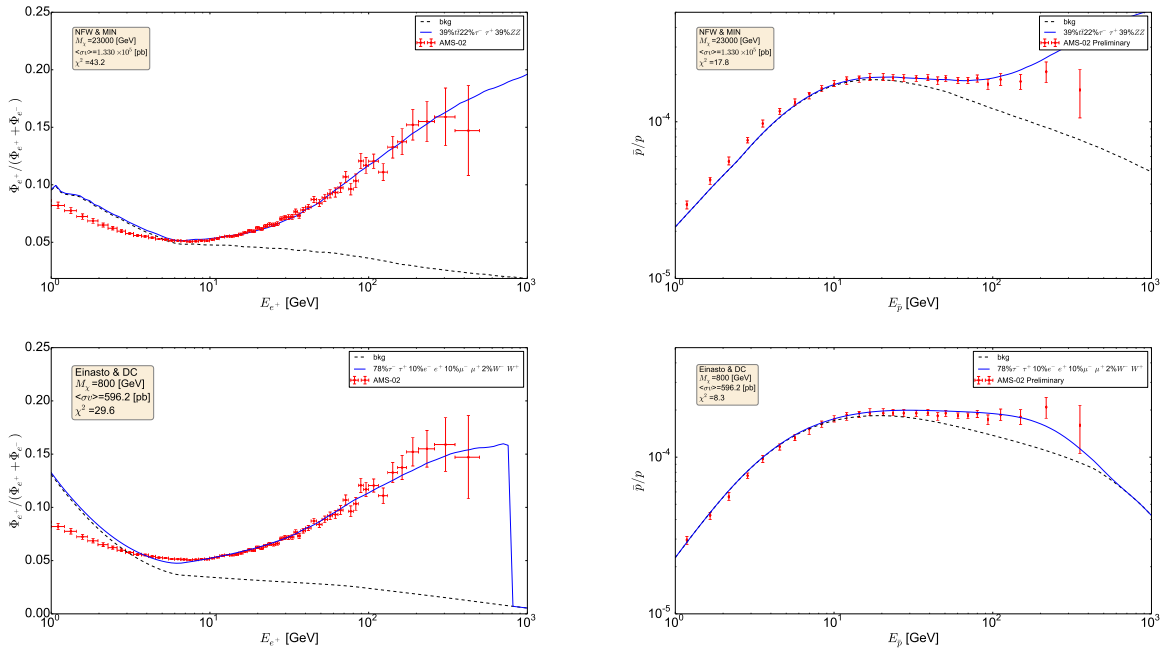


FIG. 11. The left-handed panels are for the fitting results to the AMS-02 $\frac{e^+}{e^+ + e^-}$ data, while the right-handed panels are for the fitting results to the AMS-02 $\bar{p}/p$ data. Upper two panels: under the NFW-MIN combination with a benchmark point within the compensating color region in the (M_χ, $\langle\sigma v\rangle$) panel in Fig. 4 $\Big[M_\chi = 23$ TeV, $\langle\sigma v\rangle_{tot} = 1.330 \times 10^5$ pb, Br$(\tau^+\tau^-) = 22\%$, Br$(ZZ) = 39\%$, Br$(\bar{t}t) = 39\%\Big]$. Lower two panels: under the Einasto-MED combination with a benchmark point within the red contour in the (M_χ, $\langle\sigma v\rangle$) panel in Fig. 9 $\Big[M_\chi = 800$ GeV, $\langle\sigma v\rangle_{tot} = 5.962 \times 10^2$ pb, Br$(e^+e^-) = 10\%$, Br$(\mu^+\mu^-) = 10\%$, Br$(\tau^+\tau^-) = 78\%$, Br$(W^+W^-) = 2\%\Big]$.